NeuroImage 63 (2012) 1408–1420

Contents lists available at SciVerse ScienceDirect

NeuroImage

journal homepage: www.elsevier.com/locate/ynimg

Deep brain stimulation induces BOLD activation in motor and non-motor networks: An fMRI comparison study of STN and EN/GPi DBS in large animals

Hoon-Ki Min [a], Sun-Chul Hwang [a,b], Michael P. Marsh [a], Inyong Kim [a], Emily Knight [a], Bryan Striemer [c], Joel P. Felmlee [c], Kirk M. Welker [c], Charles D. Blaha [d], Su-Youne Chang [a], Kevin E. Bennet [a,e], Kendall H. Lee [a,f,*]

[a] Department of Neurologic Surgery, Mayo Clinic, Rochester, MN, USA
[b] Department of Neurosurgery, Soonchunhyang University, Bucheon Hospital, Bucheon, Republic of Korea
[c] Department of Radiology, Mayo Clinic, Rochester, MN, USA
[d] Department of Psychology, University of Memphis, Memphis, TN, USA
[e] Division of Engineering, Mayo Clinic, Rochester, MN, USA
[f] Department of Physiology and Biomedical Engineering, Mayo Clinic, Rochester, MN, USA

ARTICLE INFO

Article history:
Accepted 4 August 2012
Available online 10 August 2012

Keywords:
Deep brain stimulation (DBS)
Parkinson's disease (PD)
Subthalamic nucleus (STN)
Globus pallidus interna (GPi)
Entopeduncular nucleus (EN)
Pedunculopontine nucleus (PPN)
Functional magnetic resonance imaging (fMRI)
Swine model
Neural circuitry

ABSTRACT

The combination of deep brain stimulation (DBS) and functional MRI (fMRI) is a powerful means of tracing brain circuitry and testing the modulatory effects of electrical stimulation on a neuronal network *in vivo*. The goal of this study was to trace DBS-induced global neuronal network activation in a large animal model by monitoring the blood oxygenation level-dependent (BOLD) response on fMRI. We conducted DBS in normal anesthetized pigs, targeting the subthalamic nucleus (STN) (n = 7) and the entopeduncular nucleus (EN), the non-primate analog of the primate globus pallidus interna (n = 4). Using a normalized functional activation map for group analysis and the application of general linear modeling across subjects, we found that both STN and EN/GPi DBS significantly increased BOLD activation in the ipsilateral sensorimotor network (FDR < 0.001). In addition, we found differential, target-specific, non-motor network effects. In each group the activated brain areas showed a distinctive correlation pattern forming a group of network connections. Results suggest that the scope of DBS extends beyond an ablation-like effect and that it may have modulatory effects not only on circuits that facilitate motor function but also on those involved in higher cognitive and emotional processing. Taken together, our results show that the swine model for DBS fMRI, which conforms to human implanted DBS electrode configurations and human neuroanatomy, may be a useful platform for translational studies investigating the global neuromodulatory effects of DBS.

Introduction

Deep brain stimulation (DBS) is a well-established restorative therapy for movement disorders, such as those associated with Parkinson's disease (PD) (Benabid, 2003; Deuschl et al., 2006), essential tremor (Benabid et al., 1993), and dystonia (Greene, 2005). The nucleus ventralis intermedius of the thalamus, the globus pallidus interna (GPi), and the subthalamic nucleus (STN) are the most frequently used DBS targets for movement disorders (Benabid et al., 1998; Krack et al., 1999).

The two most common targets for the motor symptoms of advanced PD are GPi and STN (Anderson et al., 2005; DBS-study-group, 2001). Both have been found effective for treating tremor, rigidity, and bradykinesia (Anderson et al., 2005; Benabid et al., 1994; Burchiel et al., 1999; Ghika et al., 1998; Okun and Foote, 2005), but with some notable differences. For example, GPi DBS has been found more effective than STN for treating dyskinesias (Anderson et al., 2005; Wu et al., 2001). Conversely, STN DBS appears more effective in treating severe tremor (Krack et al., 1998), akinesia (Brown et al., 1999), and for reducing dependence on dopaminergic drugs such as L-Dopa and the dyskinesias associated with its use (Krack et al., 1999; Limousin et al., 1998). Finally, adverse cognitive and behavioral effects are more frequently associated with STN than with GPi (Anderson et al., 2005; DBS-study-group, 2001; Okun and Foote, 2005).

The cognitive and psychiatric complications induced by DBS may be partly attributed to current spread into structures and substructures adjacent to the implantation site, causing unintended neural network activation (Alexander et al., 1986; Chopra et al., 2011). Both STN and GPi are key relay areas in the basal ganglia–thalamocortical circuitries, and both project to sensorimotor, limbic, and associative areas in the cortex (McIntyre and Hahn, 2010). In

* Corresponding author at: Department of Neurologic Surgery, Mayo Clinic, Rochester, Minnesota, USA.
E-mail address: lee.kendall@mayo.edu (K.H. Lee).

1053-8119
http://dx.doi.org/10.1016/j.neuroimage.2012.08.006

accordance with the classic basal ganglia model, electrical stimulation of STN and GPi should facilitate projections to these cortical areas (Kringelbach et al., 2007).

To investigate the global effects of STN and GPi DBS stimulation *in vivo*, previous studies have used fMRI or PET in conjunction with DBS stimulation in human patients who have had DBS surgery for PD. These investigations have been single-case reports or within-subject studies of motor and behavioral changes with and without DBS stimulator activation. In general, these fMRI and PET studies have found activation or, in some cases, deactivation of ipsilateral primary sensorimotor cortex, premotor cortex, the supplementary motor area, dorsolateral prefrontal cortex, the basal ganglia, the brainstem and the contralateral cerebellum (Haslinger et al., 2003; Jech et al., 2001; Phillips et al., 2006; Stefurak et al., 2003).

To better characterize the neural network and circuitry fed by STN and EN/GPi in the normal brain and to better understand the global effects of DBS, we combined DBS with fMRI studies in a large animal model, focusing on cortical as well as subcortical pathways activated by electrical stimulation. The combination of functional imaging with DBS is a powerful technique for tracing the brain's circuitry (Grafton and DeLong, 1997). For example, selective and reversible changes can be made in stimulation parameters during a single fMRI scanning session, which allows one to vary, and thus test, the modulatory potential of electricity on a subcortical–cortical pathway (Ceballos-Baumann et al., 1999; Ceballos-Baumann et al., 2001; Davis et al., 2000; Deiber et al., 1993; Haslinger et al., 2003; Jech et al., 2001; Rezai et al., 1999; Stefurak et al., 2003).

To investigate the global neuronal network effect of DBS we compared the blood oxygenation level-dependent (BOLD) response evoked by STN stimulation in anesthetized normal pigs with that evoked by stimulation of the entopeduncular nucleus (EN), which is the non-primate analog of the human GPi segment. Prior to the initiation of the experiment, we targeted the substantia nigra (SN) in a single pig for proof-of-principle.

The swine model was chosen because the large brain volume (pig brain: ~160 g) is comparable to that of the non-human primate (rhesus monkey brain: ~100 g) (Hardman et al., 2002; Shon et al., 2010), and with a gyrencephalic cortex, more closely represents human brain anatomy than do the brains of small animal models, such as rodents (Pour-El, 2006; Shon et al., 2010; Van Gompel et al., 2011; Wakeman et al., 2006). We took a novel approach using a high-resolution 3-dimensional pig brain atlas (Saikali et al., 2010), which allowed us to normalize the functional activation map and to apply general linear modeling in each subject group. This method has the advantage of permitting regression analysis for every voxel across subjects, resulting in a high statistical power that corresponds to the predictor variables (e.g., electrical stimulation parameters and target location).

Materials and methods

Animals and DBS electrode implantation

All study procedures were performed in accordance with the National Institutes of Health Guidelines for Animal Research (Guide for the Care and Use of Laboratory Animals) and approved by Mayo Clinic Institutional Animal Care and Use Committee. The subject groups consisted of 7 pigs with STN as the stimulation target and 4 pigs with EN/GPi as the stimulation target. Prior to the STN-EN/GPi comparison study, we targeted the SN in a single pig for proof of principle. The domestic male pigs weighed 30 ± 5 kg at the time of the fMRI experiment. They were fed once a day, had ad libitum access to water, and were housed individually, but with visual access to each other, in a controlled environment with humidity at 45% and temperature at 21 °C. Each subject was initially sedated with Telazol (5 mg/kg i.m.) and Xylazine (2 mg/kg i.m.), followed by intubation. Sedation was maintained with a solution of 1.5–3% isoflurane during surgery and 1.5–2% isoflurane during the fMRI experiment. The vital signs (heart rate: ~120 bpm, respiration rate:12/min, and temperature:36–37 °C) were continuously monitored throughout the procedure.

An MR image-guided stereotactic targeting system for large animals, developed by our group, was used for DBS electrode targeting and has been previously described (Fig. S1) (Shon et al., 2010). The preoperative anatomical 3D MP-RAGE image obtained for targeting was generated from a General Electric (GE) Signa HDx 3.0 Tesla (T) whole-body MRI scanner with the following parameters: repetition time (TR), 11 ms; echo time (TE), 5.16 ms; inversion time (TI), 1000 ms; flip angle (FA), 8°; slice thickness (ST), 1 mm; field of view (FOV), 24×24 mm; matrix, 256×256; slice number, 128; frequency direction (FD), A/P; Fast SPGR; ZIPx2; ZIP 512; number of excitations (NEX), 3; and acquisition time (TA), 38.20 min. A custom 3.0 T radiofrequency (RF) coil, developed in our institution's MRI RF coil laboratory specifically for this research, was used for all imaging. This fabricated RF coil is a four channel, receive-only, phased array coil with four overlapping octagon-shaped elements with each element measuring 7.3 cm in diameter. The coil array is small enough to fit just above the pig's skull inside the stereotactic head frame, a set-up that provides excellent signal-to-noise ratio. MR image-based targeting using a pig brain atlas as a reference (Felix et al., 1999; Saikali et al., 2010) was performed using COMPASS navigational software (modified for large animals) to determine the Leksell coordinates for targets STN, EN/GPi or SN and to determine a safe trajectory for delivery of the electrode (Fig. S1B). A DBS electrode (Model 3389, Medtronic Inc.) was introduced using an Alpha-Omega computer-controlled microdrive (Alpha Omega Co.). The DBS lead was secured on the skull using an anchoring system of burr hole ring and cap before being transferred from the surgical suite. Additionally, the animals were firmly secured on a carrying plate to minimize motion while moving to the MR/CT scanner. The location of the electrode was confirmed through a post-surgical CT (Dual source Somatom Definition, Siemens AG) scan (Image resolution $0.6 \times 0.6 \times 0.6$ mm) which was co-registered using a 6-parameter rigid-body transformation with the pre-MRI MP-RAGE scan (FSL, FM-RIB Analysis group) (Cho et al., 2010; Smith et al., 2004; Starr et al., 2002) (Fig. 1C).

fMRI and DBS

Following electrode implantation, subjects were transferred to the MRI scanner. For anatomical registration, 2D T2-weighted fast spin-echo (FSE) images were obtained with the following parameters: TR, 3000 ms; TE, 110 ms; FA, 90°; BW, 8.33 kHz; echo train length, 10; ST, 2.4 mm; FOV, 15×15 mm; matrix, 320×320; slice number, 32; NEX, 1; and TA, 5.07 min. fMRI was performed using a gradient echo (GRE) echo-planar imaging (EPI) pulse sequence with the following parameters: TR, 3000 ms; TE, 34.1 ms; FA, 90°; BW, 62.5 kHz; ST, 2.4 mm; FOV, 15×15 mm; matrix, 64×64; slice number, 32; FD, R/L; and TA, 12.45 min. GRE EPI integrated spatial spectral pulse was used for fat suppression. To eliminate any movement during the fMRI experiment, the pigs were administered a 2 mg bolus of pancuronium bromide, and maintained with 3 mg/h throughout the remainder of the experiment. To detect a putative BOLD signal response within the brain after electrical stimulation of either STN or EN/GPi, the following general stimulation block design was applied. After scanning 15 s (5 volumes) of discarded acquisitions to allow for scanner equilibrium, 120 s of initial scanning at rest (40 volumes of fMRI) was performed followed by five stimulus/rest blocks. These blocks each consisted of 6 s electrical stimulus (two volumes of fMRI) followed by 120 s rest (40 volumes of fMRI). This provided for a total scanning time of 12 min 45 s (255 volumes of fMRI). For STN and EN/GPi, the subjects received stimulation parameters of biphasic 1 V pulses at 130 Hz and pulse widths of 500 μs (A-M system

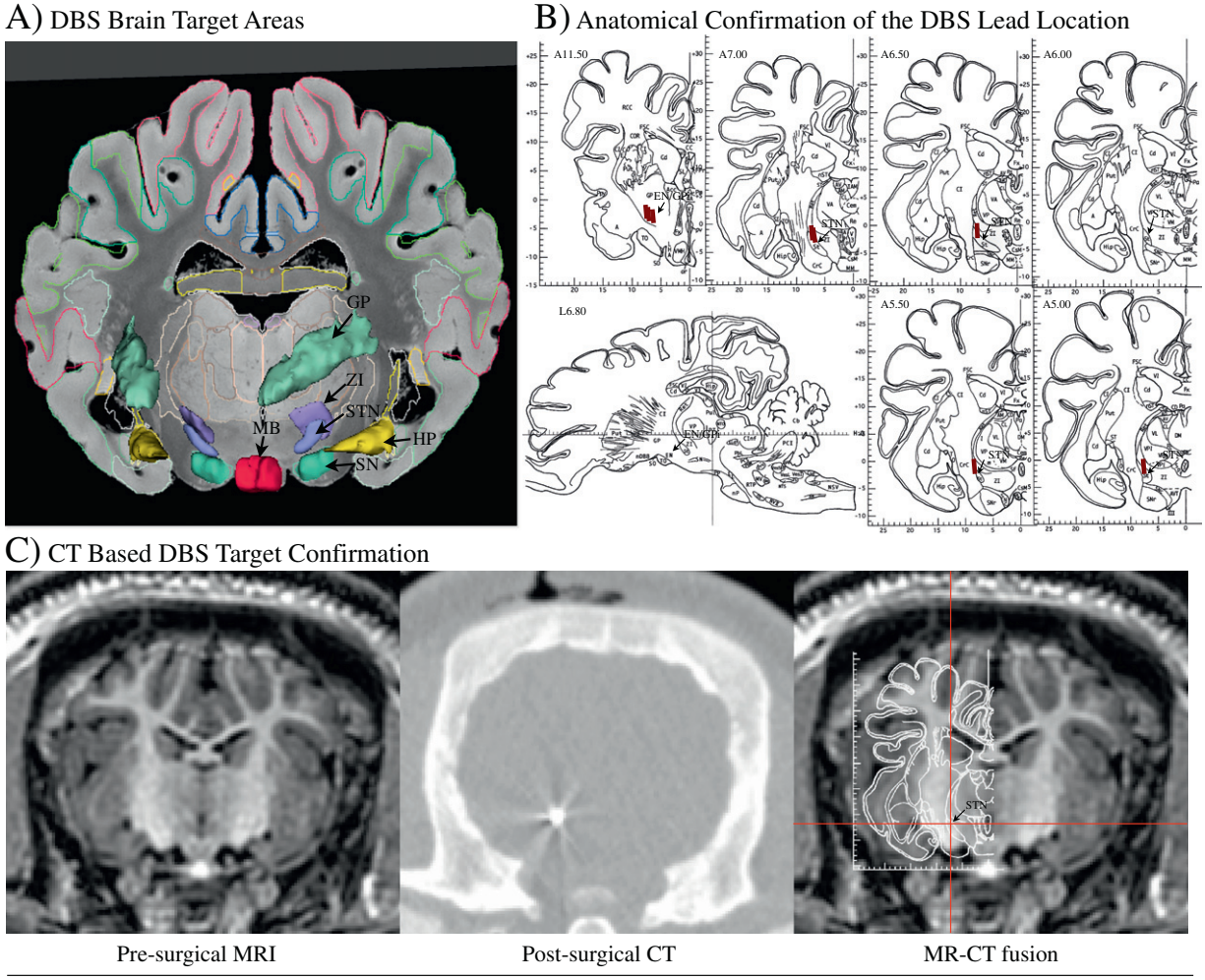

Fig. 1. DBS electrode target localization in the pig brain. A) 3D rendering of target structures (left) and atlas-based location of the STN, GP and SN (Saikali et al., 2010). B) Anatomical confirmation of the DBS lead location was marked in the pig brain atlas (Felix et al., 1999). C) Pre-surgical MRI scan (left), post-surgical CT scan (middle), and MR-CT fusion with atlas overlay demonstrating the location of the electrode tip in the STN (right). Abbreviations: GP, globus pallidus; HP, hippocampus; MB, mammillary bodies; SN, substantia nigra; STN, subthalamic nucleus; ZI, zona incerta.

isolated pulse stimulator Model 12100) using 0–1 contact of the Medtronic 3389 lead. To test the effects of stimulation intensity, 4 pigs from the STN DBS group and 3 pigs from the EN/GPi DBS group were randomly selected to receive biphasic 2 V pulses at 130 Hz and pulse widths of 500 μs followed by a ~10 min rest after the first fMRI scan. For the single subject in which SN was the target, stimulation parameters of biphasic 300 μA pulses at 60 Hz, and pulse widths of 2 ms were applied.

Anatomical confirmation of the DBS lead location

Upon completion of the experimental fMRI DBS procedure, subjects were deeply anesthetized with intravenous sodium pentobarbital (100 mg/kg) and euthanized. The brain was extracted and kept in 10% formalin for two weeks. The brain was then sectioned at 250 μm in the coronal plane by a vibratome (VT 1000 s, Leica) to confirm the DBS lead location by visual inspection of the DBS lead track. The electrode position was marked in the pig brain atlas as shown in Fig. 1B.

Data processing and analysis

The fMRI data were converted into BrainVoyager data format. A standard sequence of post-processing steps, including 3D motion correction and temporal filtering (Gaussian filter; FWHM 3 data points), was implemented in the BrainVoyager QX software and applied to each data set. Functional activation was analyzed by correlating the observed signal intensity changes in each voxel with the given stimulus protocol. Based on the results of this procedure, an appropriate activation map was generated for each subject.

To account for hemodynamic delay, the stimulus representing the block design was convolved with a double-gamma hemodynamic response function (onset 0 s, time to response peak 5 s, time to undershoot peak 15 s). To correct for multiple comparisons and exclude false positive voxels, we considered only voxels with a significance level less than the False Discovery Rate (FDR)<0.001 to represent sites of activation.

To visualize the group activation pattern during each of the five stimulation blocks, each fMRI dataset was normalized to a 3D ultra-high resolution pig brain MRI atlas (Saikali et al., 2010). Using the 2D FSE anatomical image and the first volume of the fMRI data, a manual skull and muscle stripping were performed on both 2-dimensional image leaving only the brain by Analyzer 10.0 software (Mayo Clinic) and then the image was used for a full affine (12 parameters) normalization to the 3D atlas by BrainVoyager QX.

Event-related BOLD responses were calculated by measuring the signal intensities that began 10 volumes before the stimulus onset and continued for 25 volumes after the stimulus ended. The averaged signal intensity within the appropriate area in the first 10 volumes was set to 100% signal intensity as a baseline, and post-stimulus signal variation was calculated relative to it. These datasets were then

Table 1
Areas of significant brain activation.

	Location	Size (mm3)	Coordinates (x, y, z)	Max z-score	Possible circuits involved
STN	Primary motor cortex (I)	859	5.7, 18.00, 18.9	18.73	BGTC loop (Indirect pathway), antidormic STN-cortex, DS of CST in IC
	Premotor cortex (I)	1836	2.9, 18.00, 18.1	20.40	BGTC loop (Indirect pathway), antidormic STN-cortex, DS of CST in IC
	Primary somatosensory cortex (I)	915	7.6, 30.25, 18.0	12.61	BGTC loop (Indirect pathway), antidormic STN-cortex, DS of CST in IC
	Somatosensory association cortex (I)	227	7.7, 14.50, 18.9	12.70	BGTC loop (Indirect pathway), antidormic STN-cortex, DS of CST in IC
	Dorsolateral prefrontal cortex (I)	197	4.3, 27.50, 18.0	13.20	Associative territory of STN
	Anterior Cingulate cortex (I)	634	2.9, 16.25, 14.9	17.02	Limbic territory of STN
	Insular cortex (I)	916	15.3, 30.25, 10.7	14.10	Limbic territory of STN
	Caudate nucleus (I)	142	4.5, 16.75, 7.5	7.01	STN–SNc, DS of SN, DS of NSF, PPN–SNc
	Putamen (I)	152	8.8, 20.75, −0.7	6.04	STN–SNc, DS of SN, DS of NSF, PPN–SNc
	Thalamus (I)	12	5.4, 1.75, 5.4	4.83	BGTC loop (Indirect pathway), antidormic STN–CmPf, DS of thalamus
	Pedunculopontine nucleus (I)	1	4.8, −4.25, −2.3	4.53	STN–PPN
	Prepyriform area (I)	51	18.4, 5.75, 0.2	5.07	Limbic territory of STN
	Hippocampus (I)	9	13.3, 1.75, −2.8	4.86	Limbic territory of STN
	Lateral geniculate nucleus (I)	25	10.9, −2.25, −1.4	5.56	Associative territory of STN, DS of oculomotor fiber
	Cerebellum (C)	183	−5.9, −23.00, 8.3	6.81	Motor cortex–cerebellum connection, DS of cerebello-thalamic fibers
	Temporal cortex (C)	13	−24.2, −4.25, 5.0	4.78	N/A
	Parahippocampal gyrus (C)	29	−21.0, 4.50, −3.7	5.20	N/A
EN/GPi	Primary motor cortex (I)	188	9.4, 26.5, 17.4	9.56	BGTC loop (Indirect pathway), DS of CST in IC
	Premotor cortex (I)	759	4.3, 25.50, 21.0	11.04	BGTC loop (Indirect pathway), DS of CST in IC
	Primary somatosensory cortex (I)	1175	12.7, 35.25, 14.5	11.34	BGTC loop (Indirect pathway), DS of CST in IC
	Dorsolateral prefrontal cortex (I)	220	5.7, 29.25, 18.1	10.11	Associative territory of EN/GPi
	Anterior cingulate cortex (I)	158	2.7, 19.50, 14.8	10.20	Limbic territory of EN/GPi
	Insular cortex (I)	356	14.0, 25.50, 10.1	10.47	Limbic territory of EN/GPi
	Caudate (I)	62	7.0, 24.00, 4.3	6.21	Antidormic EN/GPi-caudate
	Periaqueductal gray (C)	32	−1.0, −2.00, 0.9	5.72	N/A
	Superior colliculus (I)	1	2.8, −3.75, 3.4	4.64	DS of optic tract

Coordinates (mm): x = mediolateral, y = rostrocaudal, and z = dorsoventral. Abbreviations: BGTC, basal ganglia–thalamocortical; C, contralateral; CmPf, centromedian and parafascicular nuclei of the thalamus; CST, corticospinal tract; DS, direct stimulation through electric spread; EN, entopeduncular nucleus; GPi, globus pallidus interna; I, ipsilateral; IC, internal capsule; NSF, nigrostriatal fiber; PPN, pedunculopontine nucleus; SNc, substantia nigra pars compacta; STN, subthalamic nucleus.

further analyzed using linear regression analysis with the general linear model (GLM) and multi-subject analysis, as implemented in BrainVoyager QX software.

To investigate the pattern of relationships among the activated brain areas, regions of interest (ROI) were selected based on clusters of functional activation identified from the normalized averaged group data for each target. Pearson correlation was performed to compare the maximum signal intensity of each ROI (See Supplementary data Fig. S3). Factor analysis based on principal component analysis (PCA) with varimax rotation of the correlation matrix was then performed to identify patterns among the ROIs, and was followed by k-means clustering of the three-dimensional Eigen plot (Dunteman, 1989; Mardia et al., 1979). Agglomerative hierarchical clustering was also used to verify the number of clusters by the elbow rule (Anderberg, 1973) (Statistical Package for the Social Sciences, version 20, IBM).

Results

Stimulation of both STN (Table 1 and Fig. 2) and EN/GPi DBS (Table 1 and Fig. 3) significantly increased the BOLD signal in the ipsilateral sensorimotor network, including the premotor cortex, primary motor cortex, and primary somatosensory cortex (FDR<0.001). Group comparisons showed that there were large areas of overlap in the regions activated by these two targets. Additional areas of activation for both target sites were the ipsilateral dorsolateral prefrontal cortex, caudate nucleus, anterior cingulate cortex, and the anterior part of the insular cortex. The largest and most significant clusters of activation were detected in the sensorimotor cortex for both STN and EN/GPi DBS (Table 1).

There were also target-specific results. STN DBS was uniquely associated with activation in the ipsilateral thalamus (ventral anterior/posterior areas), the somatosensory association cortex, prepyriform area, hippocampus, lateral geniculate nuclei, pedunculopontine nucleus (PPN), the contralateral temporal cortex, parahippocampal gyrus, and cerebellum (Table 1). EN/GPi DBS was uniquely associated with periaqueductal gray and superior colliculus activation (Table 1). In the single subject experiment testing SN stimulation, DBS activated bilateral caudate nuclei, including activation of the putamen, with a stronger ipsilateral than contralateral activation. There were no regions of negative BOLD signal induced by DBS in any group. The time course representing percent change in the BOLD signal versus time demonstrated clear increases that were time-locked with each of the five blocks of stimulation pulses in each ROI (Fig. S2).

Figs. 4, A and B, show a comparison between ROI cluster sizes and the event-related time course of percent change in the BOLD signal of STN versus EN/GPi stimulation. STN stimulation resulted in larger cluster size, >30% increase than EN/GPi, which included premotor cortex, primary motor cortex, insular cortex, caudate nucleus and anterior cingulate cortex. STN stimulation also induced higher BOLD% change in the caudate than did EN/GPi ($p<0.001$, *t*-test).

Fig. 4C, shows the effects of varying stimulus intensity (1 V vs 2 V) within each group (STN DBS(n = 4) and EN/GPi DBS(n = 3)). The results showed that the size of the activated areas of the brain increased as intensity increased with STN DBS. Stimulation at 2 V (vs 1 V) generated a >30% increase in the size of the activated area, including primary somatosensory cortex, cingulate cortex, caudate, and putamen and showed a higher BOLD% change in the premotor cortex and primary motor cortex ($p<0.001$, *t*-test). A similar comparison with EN/GPi DBS, showed increased area of activation in primary somatosensory cortex, insular cortex and a decreased area of activation in prefrontal cortex. In addition, there was no significant difference in BOLD % change with EN/GPi DBS.

PCA was performed comparing each of seventeen STN ROI and nine EN/GPi ROI, defined functionally by the group analysis results in order to identify correlation patterns of the BOLD percent change in each group (Fig. 5 and Fig. S3). The PCA and subsequent cluster analysis revealed seven distinct clusters associated with STN ($p<0.001$). Cluster 1 consisted of the thalamus and PPN. Cluster 2 consisted of the caudate nucleus, putamen, and prepyriform area. Cluster 3 consisted of primary motor cortex, lateral geniculate nuclei, and cerebellum. Cluster 4 consisted of parahippocampal gyrus. Cluster 5 consisted of primary somatosensory cortex, somatosensory association cortex, and insular cortex. Cluster 6 consisted of premotor cortex, anterior cingulate cortex

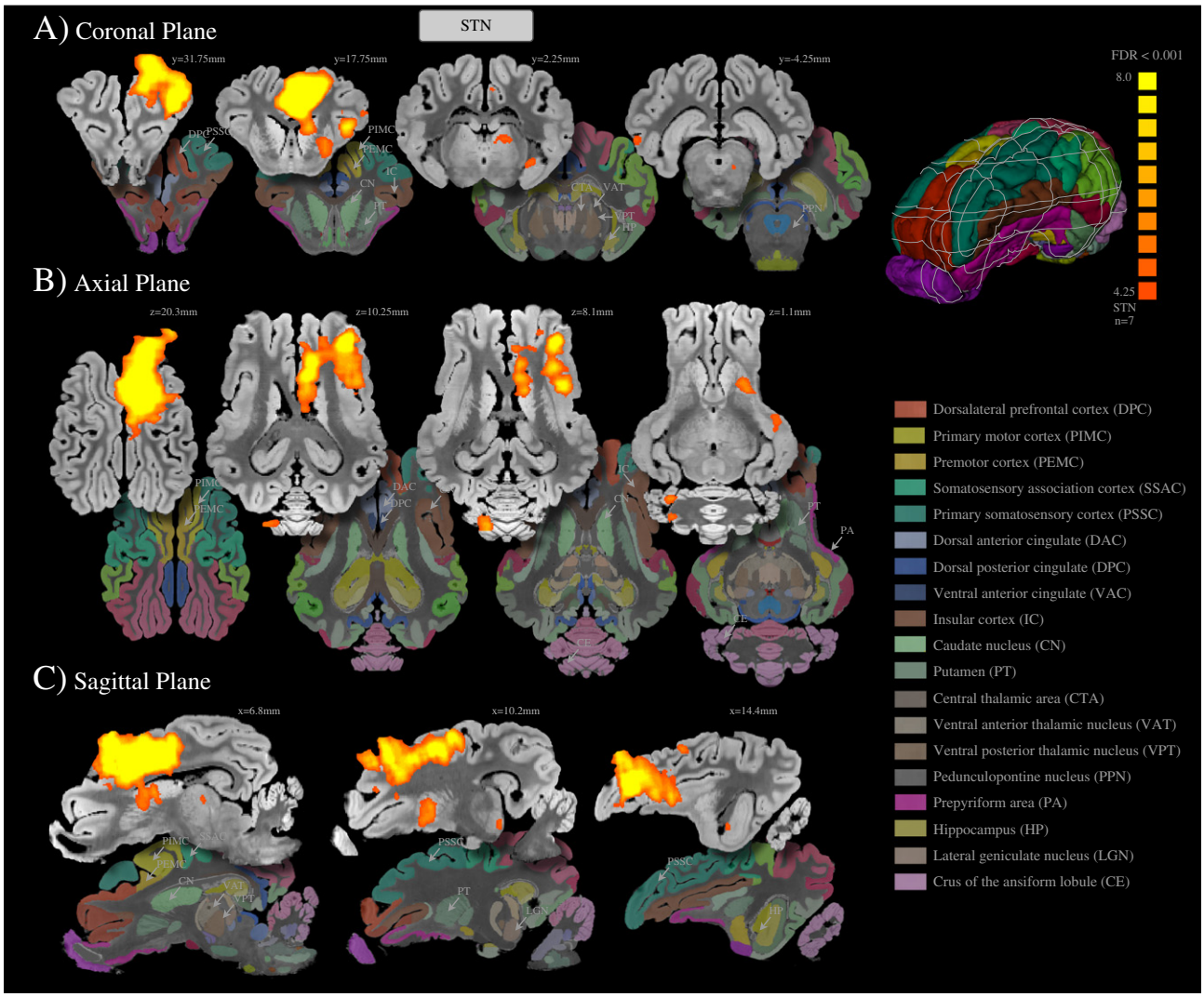

Fig. 2. Areas of activation with STN stimulation at 1 V 130 Hz 0.5 ms, normalized to a 3D pig brain template (Saikali et al., 2010). Significant activation (FDR<0.001) was observed in the ipsilateral premotor cortex, primary motor cortex, primary somatosensory cortex, dorsolateral prefrontal cortex, caudate nucleus, putamen, anterior cingulate cortex, insular cortex, thalamus (central, ventral anterior and ventral posterior areas), prepyriform area, hippocampus, lateral geniculate nucleus, pedunculopontine nucleus, and the contralateral cerebellum.

and the hippocampus. Cluster 7 consisted of dorsolateral prefrontal cortex and temporal cortex (Fig. 5A).

EN/GPi DBS PCA revealed five clusters ($p<0.05$). Clusters 1 and 2, with one component each, consisted of periaqueductal gray and primary motor cortex, respectively. Cluster 3 consisted of caudate and insular cortex. Cluster 4 consisted of primary sensory cortex and dorsolateral prefrontal cortex. Cluster 5 consisted of premotor cortex, anterior cingulate cortex, and superior colliculus (Fig. 5B).

Discussion

Our results show significant activation in the ipsilateral premotor cortex, primary motor cortex, primary somatosensory cortex, dorsolateral prefrontal cortex, head of the caudate, anterior cingulate cortex, and insular cortex with both STN and EN/GPi stimulation. Combined with previous findings, our data support the theory that DBS has a neuromodulatory effect, which facilitates the basal ganglia–thalamocortical loop complex in modulating global neural activity in both motor and non-motor circuits (Grill et al., 2004; Kringelbach et al., 2007; McIntyre et al., 2004a; McIntyre et al., 2004b; Vitek, 2002b) (See Table 2).

The activation of premotor, primary motor and sensory cortices by both STN and EN/GPi DBS supports the sensorimotor network as the basis for the common therapeutic effect of these two targets in the treatment of PD. Compared to EN/GPi DBS, STN DBS was shown on fMRI to recruit a larger area of the motor network. This finding is in concert with the suggestion that STN DBS is a superior target for improving motor performance scores (DBS-study-group, 2001). Of note, our study was not a within-subject design, and the group comparison results may have been affected by the unequal number of subjects per group (4 vs 7). However, our data shows that activation patterns in individual subjects conform well to the group data. The difference in activation found between STN and GPi DBS may be related in part to the physical size difference of GPi compared to STN. The anatomical size of GPi is larger than STN, and the use of an identical stimulation parameter could thus have induced greater electrical stimulation effects for STN DBS compared to GPi DBS. Our voltage comparison results (Fig. 4C) suggest that STN is more sensitive than EN/GPi to stimulation intensity. This discrepancy has been demonstrated in the clinical setting in which GPi DBS requires a higher charged density parameter (higher voltage) than does STN-DBS to produce the same therapeutic outcome(Anderson et al., 2005; Okun and Foote, 2005). However, because the outcome can be optimized by changing stimulation contacts and/or stimulation parameters, both STN and GPi are considered appropriate therapeutic targets for DBS, as shown recently in a randomized clinical study on the motor symptoms associated with PD (Anderson et al., 2005).

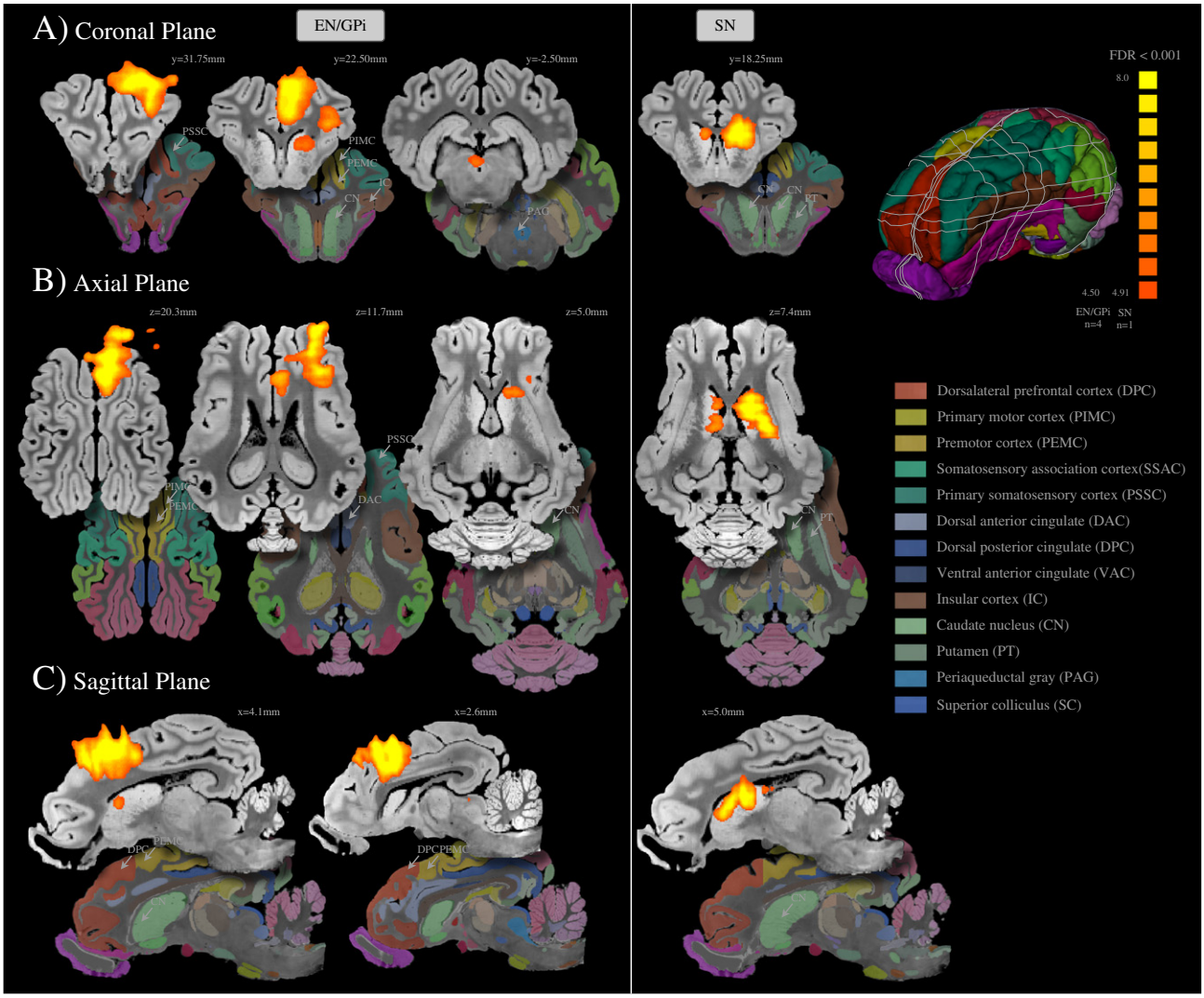

Fig. 3. Areas of activation with EN/GPi stimulation at 1 V 130 Hz 0.5 ms (left) and SN stimulation at 300 mA 60 Hz 2 ms (right), normalized to a 3D pig brain template (left) (Saikali et al., 2010). With EN/GPi stimulation, significant activation (FDR<0.001) was observed in the ipsilateral premotor cortex, primary motor cortex, primary somatosensory cortex, dorsolateral prefrontal cortex, caudate nucleus, anterior cingulate cortex, insular cortex, and contralateral periaqueductal gray. SN stimulation activated ipsilateral and contralateral caudate nucleus and ipsilateral putamen.

Of note, although the pig brain is closer in volume and structure to the human brain than the rodent brain, there are marked differences between pigs and humans in the volume of both STN and GPi/EN. The volume of STN is 0.8 ± 0.1 mm^3 in the rat, 50 ± 7 mm^3 in the pig, 34 ± 6 mm^3 in the Macaque monkey, and 240 ± 23 mm^3 in the human. The volume of EN/GPi is 2.2 ± 0.7 mm^3 in the rat, ~180 mm^3 in the pig, 127 ± 26 mm^3 in the Macaque, and 957 ± 209 mm^3 in the human (Felix et al., 1999; Hardman et al., 2002; Saikali et al., 2010; Shon et al., 2010). We took several steps to accommodate these volumetric differences. We used a human DBS electrode with low voltage (1 V) and long pulse duration (500 μsec) in an effort to increase current density while containing the spread of the electrical field (Kringelbach et al., 2007; Lozano et al., 2002). Each DBS electrode has four contact points. The Medtronic 3389 DBS electrode used in this study has smaller gap (0.5 mm) between contact points than the Medtronic 3387 electrode, which has a gap of 1.5 mm and is commonly used for human DBS surgery in North America. In addition, we stimulated only the 0–1 contact. Nonetheless, given the small size of the swine STN and EN/GPi, it is likely that we activated the entire STN and EN/GPi and partly surrounding areas in the pig brain. However, as Fig. 5 shows, the activated areas for each target revealed a specific correlation pattern, which suggests a distinct set of network connections.

Other sources of variance in this study include consistency of targeting and the influence of the stimulation block-design. As is true of any electrode implantation study, anatomic variations across subjects can translate into small variations in the precise position of the stimulating electrode. In addition, while stimulations within a stimulation-block may have been independent, it may also have influenced the succeeding stimulations (see Supplementary data Fig. S2). This potential composite stimulation effect could cause fluctuations in the brain areas that are activated. These inter- and intra-subject sources of variance make the correlations shown in Fig. 5 even more notable, given the strong correlations among activated areas and the resulting consistent, integrated networks they appear to define for each target.

Obtaining optimal clinical benefit from DBS requires maximal coverage of the targeted subcortical region by the stimulation fields while minimizing current spread to adjacent structures that may induce adverse side-effects (Kringelbach et al., 2007; Montgomery and Gale, 2008). Thus, it is of note that, despite some current spread, we nonetheless found differential, target-specific non-motor network effects. The PCA analysis for STN revealed distinct correlation patterns, each comprising functional connectivity between ROI. Clusters 1 and 2 consisted of brain areas that may represent the basal ganglia–thalamocortical network, including the putamen, caudate

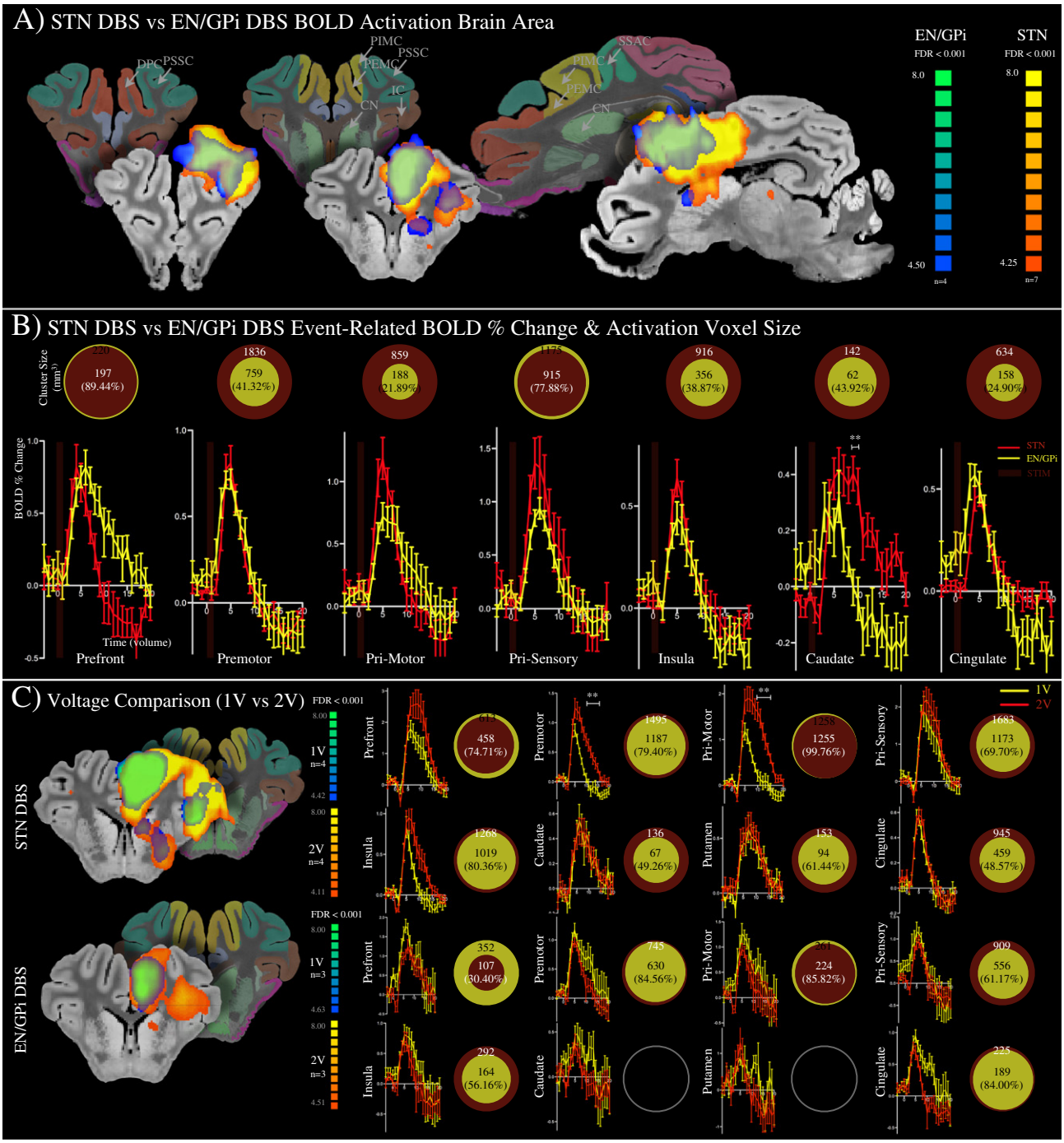

Fig. 4. A) The fMRI activation map of STN (red scale) and EN/GPi (blue scale) DBS fMRI activation map. Areas of overlap include dorsolateral prefrontal cortex, premotor cortex, primary motor cortex, primary somatosensory cortex, insula cortex, caudate and anterior cingulate cortex. B) Region of interest cluster sizes (top) and event-related time course of percent change in BOLD signal from baseline (bottom) with STN stimulation (red) versus EN/GPi stimulation (yellow). STN stimulation resulted in greater area of activation of premotor cortex, primary motor cortex, insular cortex, caudate and anterior cingulate cortex than EN/GPi stimulation. STN also showed higher BOLD activation in the Caudate ($p<0.001$, *t*-test). C) Voltage comparison showing fMRI activation map of 1 V (blue scale) and 2 V (red scale) of each group. Region of interest cluster sizes and event-related time course of percent change in BOLD signal have been compared (1 V-yellow vs 2 V-red).

nucleus, and thalamus. Clusters 3 and 5 consisted of brain areas representing the sensorimotor network, including primary motor cortex, cerebellum, primary somatosensory cortex, and sensory association cortex. Clusters 4, 6, and 7 consisted of brain areas representing the cognitive/emotional network, including the anterior cingulate cortex, hippocampus, dorsolateral prefrontal cortex and temporal cortex. Although our results also revealed clustering of EN/GPi DBS brain areas, the pattern that emerged did not share characteristics with any known neural-network pattern.

The regional connections found in this study may also shed light on the growing body of evidence that suggests DBS for PD can induce psychiatric complications. Among the known adverse effects, which can include suicide (Appleby et al., 2007; Funkiewiez et al., 2004), are depression(Bejjani et al., 1999; Berney et al., 2002; Doshi et al., 2002; Houeto et al., 2002), hypomania, euphoria, impulsivity and hypersexuality (Burn and Troster, 2004; Chopra et al., 2011; Frank et al., 2007; Herzog et al., 2003; Krack et al., 2001; Kulisevsky et al., 2002; Romito et al., 2002; Witt et al., 2008). These complications are most often

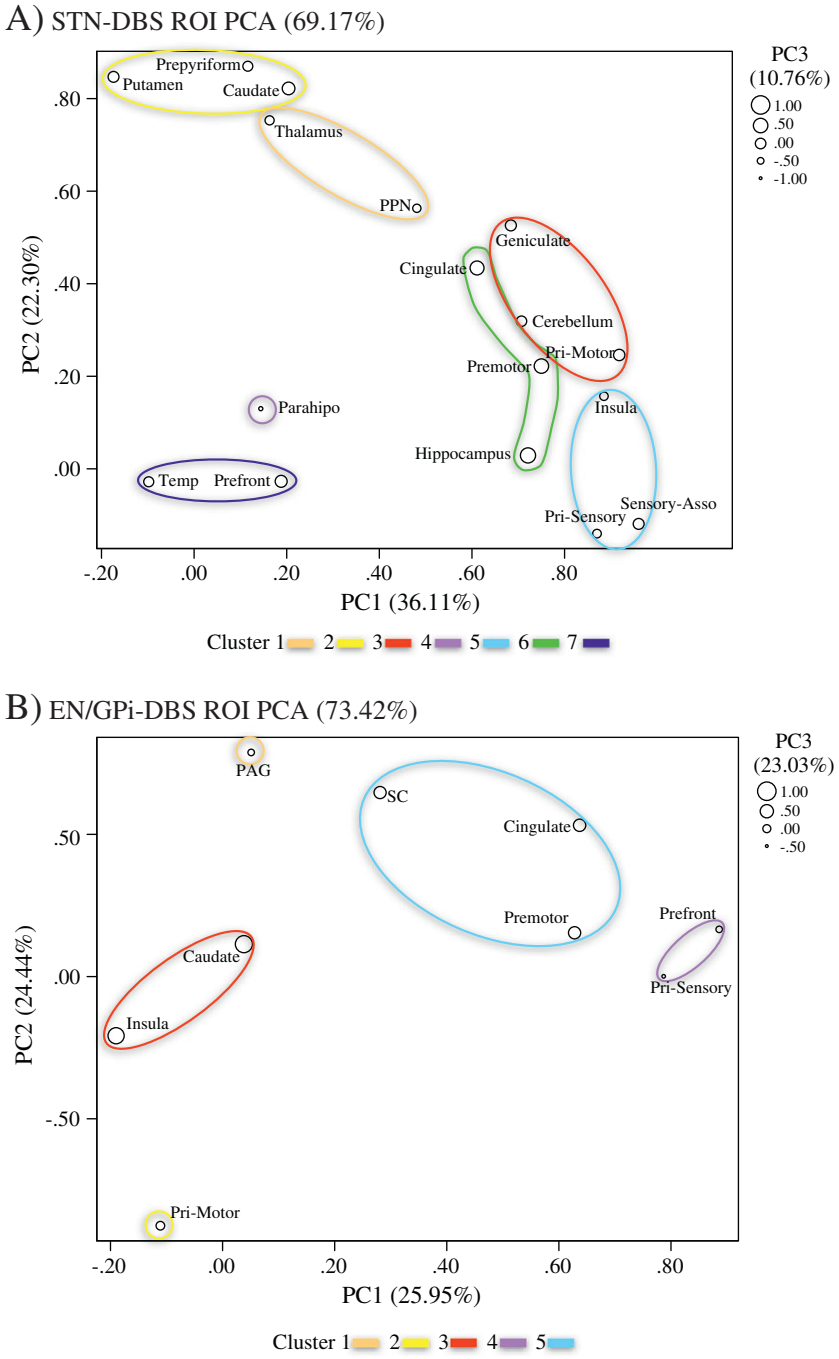

Fig. 5. Principal component analysis between functionally-defined regions of interest for STN (A) and EN/GPi (B) DBS. Additional cluster analysis revealed seven groups for STN DBS and five groups for EN/GPI, which are outlined in circles. For STN DBS clusters 1 and 2 consist of brain areas that represent the basal ganglia–thalamocortical network. Clusters 3 and 5 consist of brain areas representing the sensorimotor network. Clusters 4, 6, and 7 consist of brain areas representing the cognitive/emotional network. EN/GPi DBS pattern that emerged did not share characteristics with any known neural-network pattern.

associated with STN (versus GPi) DBS (Anderson and Mullins, 2003; Burn and Troster, 2004; Fields et al., 1999; Herzog et al., 2003; Kulisevsky et al., 2002; Miyawaki et al., 2000; Saint-Cyr et al., 2000; Tarsy, 2008; Trepanier et al., 2000; Vingerhoets et al., 1999; Vitek, 2002a; Voon et al., 2006).

Functional neuroimaging studies have shed light on the involvement of non-motor circuits in the cognitive effects and pathophysiology of PD. Metabolic decrease in the left orbitofrontal cortex and dorsal anterior cingulate, for example, has been associated with a decline in verbal learning. Decreased verbal fluency associated with FDG uptake in the left dorsolateral prefrontal cortex and right dorsal anterior cingulate following STN DBS has also been reported (Kalbe et al., 2009). Reduced gray matter density in the insular cortex and cingulate has been linked to apathy in PD (Reijnders et al., 2010). Finally, white matter loss in the cingulate and orbitofrontal cortex is associated with depression in PD (Kostic et al., 2010).

An early human fMRI DBS case study with fMRI results similar to our STN results, reported both mood and motor responses induced by STN DBS. In a patient with PD, left DBS improved motor symptoms. However, unexpectedly, right DBS elicited several reproducible episodes of acute depressive dysphoria. The fMRI data revealed that left DBS primarily affected motor regions, which included increased activation of

Table 2
Anatomical connections of STN and EN/GPi.

	Category	Locations	Structures	Connections	Functions/adverse event (DBS)
STN	Substructures	Dorsolateral	Motor area	A: Motor and Premotor cortices (Glu)	F: 'indirect' pathway of BGTC projection
				A: GPe (GABA)	F: 'indirect' pathway of BGTC projection
				E: GPi, GPe, and SNr (Glu)	F: 'indirect' pathway of BGTC projection
		Ventromedial	Associative area	A: Dorsolateral prefrontal cortex	F: Oculomotor control and cognitive aspects of motor behavior
				A: Frontal eye field	F: Oculomotor control and cognitive aspects of motor behavior
				E: SNr	F: Oculomotor control and cognitive aspects of motor behavior
		Medial	Limbic area	A: Medial prefrontal cortex	F: Motivational and emotional aspects of motor behavior
				A: Anterior cingulate cortex	F: Motivational and emotional aspects of motor behavior
				E: Ventral and medial pallidum	F: Motivational and emotional aspects of motor behavior
	Other connections			A: CmPf (Glu)	
				R: PPN (A: Glu and Cho, E: Glu)	F: Controlling motor pattern generators (Gait)
				R: SNc	
	Surrounding structures	Posterior-medial and dorsal	Thalamus and medial lemniscus		AE: Persistent dyesthesias
		Lateral and a	IC (corticobulbar fiber)		AE: Dysarthria/dysphagia
			IC (corticospinal fiber)		AE: Tonic muscle contraction
		Ventral	SN		AE: Acute depression
		Dorsal	ZI and the H2 FF (includes MFB)		
		Medial and ventral	Oculomotor fibers		AE: Diplopia/eye deviations
			Cerebello-thalamic fibers		AE: Diplopia/eye deviations
					AE: Ataxia
		Posteromedial	Red nucleus		
EN/GPi	Substructures	Posteroventral	Sensorimotor area	A: GPe (GABA)	
				A: STN (Glu)	
				E: VA nucleus of the thalamus (GABA)	
				E: VL nucleus of the thalamus (GABA)	
		Dorsal	Associative area		AE: Relief of akinesia but no relief of dyskinesia
		Ventromedial	Limbic area		AE: Relief of dyskinesia and rigidity but worse akinesia
	Other connections			E: CmPf (GABA)	
				E: Lateral habenular nucleus (GABA)	
				E: PPN	
	Surrounding structures	Anterior	Anterior commissure		
		Ventral	Optic tract		AE: Visual phenomena
		Medial and posterior	IC (corticobulbar fiber)		AE: Dysarthria
			IC (corticospinal fiber)		AE: Tonic muscle contraction

Abbreviations: A, afferent connection; AE; adverse event; BGTC, basal ganglia–thalamocortical; Cho, cholinergic; CmPf, centromedian and parafascicular nuclei of the thalamus; E, efferent connection; EN, entopeduncular nucleus; F, functions; FF, feild of forel; GABA, -Aminobutyric acid; Glu, glutamatergic; GPe, globus pallidus externa; GPi, globus pallidus interna; IC, internal capsule; MFB, medial forebrain bundle; PPN, pedunculopontine nucleus; R, reciprocal connection; SN, substantia Nigra; SNc, substantia nigra pars compacta; SNr, substantia nigra pars reticulata; STN, subthalamic nucleus; VA, ventral anterior; VL, ventral lateral; ZI, zona incerta (Benarroch, 2008; Tarsy, 2008).

premotor and motor cortex, ventrolateral thalamus, putamen, and cerebellum, as well as decreased activation of sensorimotor/supplementary motor cortex. Right DBS showed similar but less extensive changes in motor regions. More prominent were the unique increases in the superior prefrontal cortex, anterior cingulate, anterior thalamus, caudate, and brainstem, with marked and widespread decreases in medial prefrontal cortex activation (Stefurak et al., 2003).

A PET study of two patients with PD who underwent DBS surgery revealed additional non-motor effects of STN stimulation (Mallet et al., 2007). Selective stimulation of subterritories of the STN with simultaneous PET assessment of cortical activation showed that with a target localized in the anteromedial STN, stimulation of the anteromedial contact and the contact immediately dorsal to it not only led to a reduction in motor symptoms, but also consistently produced a hypomanic state. This state was likely mediated by the activation of limbic and association cortex, including areas of the anterior cingulate gyrus and ventral anterior nucleus of the thalamus (Benarroch, 2008; Mallet et al., 2007).

A recent clinical report showed that using model-based optimization of DBS stimulation parameters to avoid current spread to non-motor areas reduced cognitive and cognitive–motor impairments while maintaining therapeutic motor benefit (Frankemolle et al., 2010). Our data suggest that anatomical target placement decisions during human DBS surgery could be augmented by consideration of the functional consequences of STN stimulation on non-motor cortical areas, which, from our results, appear to be part of an electrically influenced STN neural network.

In our study, STN stimulation induced greater activation in the caudate and putamen than EN/GPi. This finding may help to explain why more patients have been able to reduce medication dosage following STN DBS than following GPi DBS (Benabid et al., 1994; DBS-study-group, 2001; Kumar et al., 1998). In previous studies we have shown that electrical stimulation of the STN in the rat induces excitatory postsynaptic potentials in substantia nigra pars compacta (SNc) dopaminergic neurons in vitro (Lee et al., 2003; Lee et al., 2004) and increased striatal dopamine release *in vivo* (Lee et al., 2006). We have also found that STN DBS in pigs evokes intensity- and frequency-dependent striatal dopamine release (Shon et al., 2010). While it appears that both medication reduction and improved motor performance are consistent with STN DBS in humans, it may be that increased dopamine release produces dopaminergic-related behavioral complications such as impulse control disorders (Broen et al., 2011).

It is well-known that the STN has reciprocal interactions with the dopaminergic neurons of the SNc. The STN, both directly and indirectly, via the PPN conveys excitatory influence from prefrontal cortex to these dopaminergic neurons, which is critical for their reward-related activity (Benarroch, 2008) (See Table 2). For example, a case report of a patient with PD found that ventral STN DBS induced manic symptoms which resolved with dorsolateral STN stimulation (Ulla et al., 2006). The report suggested that the patient's mania was induced by dopaminergic circuit stimulation. We, too, have reported on a patient with PD in whom STN DBS generated a voltage-dependent mania, possibly due to electrical spread (Chopra et al., 2011). However, a series of [C-11] raclopride PET studies in PD patients failed to demonstrate any changes in synaptic dopamine release induced by DBS (Abosch et al., 2003; Hilker et al., 2003; Strafella et al., 2003). Thus the role of dopamine in DBS remains unclear and warrants further study.

Current postoperative DBS pulse generator programming decisions are based on and limited by the subjective judgments of the patient and the stimulus programmer. It has been reported that more than one-third of patients referred to two specialized movement disorder centers for "DBS failures" were not properly programmed (Okun et al., 2005). Given the potential for fMRI to reveal distal activation from DBS, we envision it could be a useful adjunct for objectively determining and evaluating programming parameters after DBS surgery (Kringelbach et al., 2007). We also recognize that it is important to keep in mind safety precautions when using fMRI with DBS, predominant among which is the increase in temperature near the electrode tips from the scanner RF field focusing (Baker et al., 2007; Carmichael et al., 2007; Phillips et al., 2006; Pictet et al., 2002; Rezai et al., 2002; Rezai et al., 2005).

We recognize several limitations of the present study. In our data, the frontal sinus of the pig brain is thought to cause a geometric distortion in the EPI image, which is limited to rostral part of the prefrontal cortex and anterior part of the primary somatosensory cortex. Thus, some activated brain regions in the frontal cortex were outside of the atlas borders. However, although this MRI distortion could have caused an error in the voxel-based analysis, especially in prefrontal cortex, it is of note that it is limited to the tissue-air interfaces and thus unlikely to affect other brain areas (Jezzard and Clare, 1999).

We also recognize that our STN DBS vs GPi DBS comparison is not a within-subject design using within-scan comparison. Therefore more sophisticated fMRI experiments would be needed in the future to further evaluate the question of clinical therapeutic effects vs side effects of STN vs GPi DBS. This question remains a matter of considerable debate (Green et al., 2006; Moum et al., 2012; Okun and Foote, 2005; Weaver et al., 2012).

In addition, to better accommodate the small size of the pig STN and EN/GPi, rather than using a human DBS electrode, we plan to use miniaturized DBS leads (Miocinovic et al., 2007). We also envision that a more sophisticated lead design (Chaturvedi et al., 2012; Martens et al., 2011) and a selective neuronal activation method, such as optogenetic stimulation (Kravitz et al., 2010; Lee, 2012), which can be combined with neuroimaging would allow enhanced discrimination of the global neuromodulary network effects of neural stimulation.

Functional neuroimaging is extremely difficult in the conscious animal. Although awake fMRI might yield different results from those in the anesthetized state, and our use of sedation and muscle relaxant was based on previous animal fMRI studies which showed robust visual and electrical stimulation-dependent BOLD responses and electrophysiological responses in the anesthetized state (Angenstein et al., 2009; Angenstein et al., 2010; Jin and Kim, 2008; Masamoto et al., 2007).

In the present study, we used an acute protocol in a non-PD animal model, which enabled both proof of principle and an investigation of the effects of neural network electrical stimulation on the normally functioning swine brain model. We have recently confirmed our MR image-guided targeting system and fMRI group analysis method in Yucatan minipigs (data not included) for which there is a PD model available (Bjarkam et al., 2008; Nielsen et al., 2009). The work reported here, thus sets the stage for future investigations that combine functional neuroimaging with electrical stimulation in a chronic MPTP (1-methyl-4-phenyl-1,2,3,6-tetrahydropyridine) PD model.

Conclusions

Our findings suggest that DBS at both targets increased BOLD activation at a number of subcortical and cortical projection areas within the basal ganglia–thalamocortical network. The activated brain areas shown in our data reflect an effect of electrical stimulation spreading via orthodromic and/or antidromic activation for each DBS target. While STN and EN/GPi stimulation showed common sensorimotor network activation, our correlation data suggest that each target also activates a distinctive neural network. Taken together our results support the differences and similarities between STN and GPi noted in clinical reports comparing the two targets. The results also suggest that the swine model for DBS fMRI, which conforms to human implanted DBS electrode configurations and human neuroanatomy, may be a useful platform for translational studies investigating the global neuromodulatory effects of DBS.

Acknowledgments

This work was supported by The Grainger Foundation, and by the National Institutes of Health (K08 NS 52232 and R01 NS 70872 to KHL). The authors are grateful to Penelope Duffy, Ph.D. for her editorial contributions and review. We thank Dr. Stephan Saikali and Dr. Charles Henri Malbert for their public release of their 3D ultra-high resolution pig brain atlas. We also thank Osama Abulseoud, M.D. for his assistance with the psychiatric portions of the Discussion and the Center for Advanced Imaging Research, Opus Building, Mayo Clinic for their support.

Appendix A. Supplementary data

Supplementary data to this article can be found online at http://dx.doi.org/10.1016/j.neuroimage.2012.08.006.

References

Abosch, A., Kapur, S., Lang, A.E., Hussey, D., Sime, E., Miyasaki, J., Houle, S., Lozano, A.M., 2003. Stimulation of the subthalamic nucleus in Parkinson's disease does not produce striatal dopamine release. Neurosurgery 53, 1095–1102 (discussion 1102–1095).

Alexander, G.E., DeLong, M.R., Strick, P.L., 1986. Parallel organization of functionally segregated circuits linking basal ganglia and cortex. Annu. Rev. Neurosci. 9, 357–381.

Anderberg, M.R., 1973. Cluster Analysis for Applications. Academic Press, New York.

Anderson, K.E., Mullins, J., 2003. Behavioral changes associated with deep brain stimulation surgery for Parkinson's disease. Curr. Neurol. Neurosci. Rep. 3, 306–313.

Anderson, V.C., Burchiel, K.J., Hogarth, P., Favre, J., Hammerstad, J.P., 2005. Pallidal vs subthalamic nucleus deep brain stimulation in Parkinson disease. Arch. Neurol. 62, 554–560.

Angenstein, F., Kammerer, E., Scheich, H., 2009. The BOLD response in the rat hippocampus depends rather on local processing of signals than on the input or output activity. A combined functional MRI and electrophysiological study. J. Neurosci. Off. J. Soc. Neurosci. 29, 2428–2439.

Angenstein, F., Krautwald, K., Scheich, H., 2010. The current functional state of local neuronal circuits controls the magnitude of a BOLD response to incoming stimuli. NeuroImage 50, 1364–1375.

Appleby, B.S., Duggan, P.S., Regenberg, A., Rabins, P.V., 2007. Psychiatric and neuropsychiatric adverse events associated with deep brain stimulation: a meta-analysis of ten years' experience. Mov. Disord. 22, 1722–1728.

Baker, K.B., Kopell, B.H., Malone, D., Horenstein, C., Lowe, M., Phillips, M.D., Rezai, A.R., 2007. Deep brain stimulation for obsessive-compulsive disorder: using functional magnetic resonance imaging and electrophysiological techniques: technical case report. Neurosurgery 61, E367–E368 (discussion E368).

Bejjani, B.P., Damier, P., Arnulf, I., Thivard, L., Bonnet, A.M., Dormont, D., Cornu, P., Pidoux, B., Samson, Y., Agid, Y., 1999. Transient acute depression induced by high-frequency deep-brain stimulation. N. Engl. J. Med. 340, 1476–1480.

Benabid, A.L., 2003. Deep brain stimulation for Parkinson's disease. Curr. Opin. Neurobiol. 13, 696–706.

Benabid, A.L., Pollak, P., Seigneuret, E., Hoffmann, D., Gay, E., Perret, J., 1993. Chronic VIM thalamic stimulation in Parkinson's disease, essential tremor and extrapyramidal dyskinesias. Acta Neurochir. Suppl. (Wien) 58, 39–44.

Benabid, A.L., Pollak, P., Gross, C., Hoffmann, D., Benazzouz, A., Gao, D.M., Laurent, A., Gentil, M., Perret, J., 1994. Acute and long-term effects of subthalamic nucleus stimulation in Parkinson's disease. Stereotact. Funct. Neurosurg. 62, 76–84.

Benabid, A.L., Benazzouz, A., Hoffmann, D., Limousin, P., Krack, P., Pollak, P., 1998. Long-term electrical inhibition of deep brain targets in movement disorders. Mov. Disord. 13 (Suppl. 3), 119–125.

Benarroch, E.E., 2008. Subthalamic nucleus and its connections: anatomic substrate for the network effects of deep brain stimulation. Neurology 70, 1991–1995.

Berney, A., Vingerhoets, F., Perrin, A., Guex, P., Villemure, J.G., Burkhard, P.R., Benkelfat, C., Ghika, J., 2002. Effect on mood of subthalamic DBS for Parkinson's disease: a consecutive series of 24 patients. Neurology 59, 1427–1429.

Bjarkam, C.R., Nielsen, M.S., Glud, A.N., Rosendal, F., Mogensen, P., Bender, D., Doudet, D., Moller, A., Sorensen, J.C., 2008. Neuromodulation in a minipig MPTP model of Parkinson disease. Br. J. Neurosurg. 22 (Suppl. 1), S9–S12.

Broen, M., Duits, A., Visser-Vandewalle, V., Temel, Y., Winogrodzka, A., 2011. Impulse control and related disorders in Parkinson's disease patients treated with bilateral subthalamic nucleus stimulation: a review. Parkinsonism Relat. Disord. 17, 413–417.

Brown, R.G., Dowsey, P.L., Brown, P., Jahanshahi, M., Pollak, P., Benabid, A.L., Rodriguez-Oroz, M.C., Obeso, J., Rothwell, J.C., 1999. Impact of deep brain stimulation on upper limb akinesia in Parkinson's disease. Ann. Neurol. 45, 473–488.

Burchiel, K.J., Anderson, V.C., Favre, J., Hammerstad, J.P., 1999. Comparison of pallidal and subthalamic nucleus deep brain stimulation for advanced Parkinson's disease: results of a randomized, blinded pilot study. Neurosurgery 45, 1375–1382 (discussion 1382–1374).

Burn, D.J., Troster, A.I., 2004. Neuropsychiatric complications of medical and surgical therapies for Parkinson's disease. J. Geriatr. Psychiatry Neurol. 17, 172–180.

Carmichael, D.W., Pinto, S., Limousin-Dowsey, P., Thobois, S., Allen, P.J., Lemieux, L., Yousry, T., Thornton, J.S., 2007. Functional MRI with active, fully implanted, deep brain stimulation systems: safety and experimental confounds. NeuroImage 37, 508–517.

Ceballos-Baumann, A.O., Boecker, H., Bartenstein, P., von Falkenhayn, I., Riescher, H., Conrad, B., Moringlane, J.R., Alesch, F., 1999. A positron emission tomographic study of subthalamic nucleus stimulation in Parkinson disease: enhanced movement-related activity of motor-association cortex and decreased motor cortex resting activity. Arch. Neurol. 56, 997–1003.

Ceballos-Baumann, A.O., Boecker, H., Fogel, W., Alesch, F., Bartenstein, P., Conrad, B., Diederich, N., von Falkenhayn, I., Moringlane, J.R., Schwaiger, M., Tronnier, V.M., 2001. Thalamic stimulation for essential tremor activates motor and deactivates vestibular cortex. Neurology 56, 1347–1354.

Chaturvedi, A., Foutz, T.J., McIntyre, C.C., 2012. Current steering to activate targeted neural pathways during deep brain stimulation of the subthalamic region. Brain Stimul. 5, 369–377.

Cho, Z.H., Min, H.K., Oh, S.H., Han, J.Y., Park, C.W., Chi, J.G., Kim, Y.B., Paek, S.H., Lozano, A.M., Lee, K.H., 2010. Direct visualization of deep brain stimulation targets in Parkinson disease with the use of 7-tesla magnetic resonance imaging. J. Neurosurg. 113, 639–647.

Chopra, A., Tye, S.J., Lee, K.H., Matsumoto, J., Klassen, B., Adams, A.C., Stead, M., Sampson, S., Kall, B.A., Frye, M.A., 2011. Voltage-dependent mania after subthalamic nucleus deep brain stimulation in Parkinson's disease: a case report. Biol. Psychiatry 70, e5–e7.

Davis, K.D., Taub, E., Duffner, F., Lozano, A.M., Tasker, R.R., Houle, S., Dostrovsky, J.O., 2000. Activation of the anterior cingulate cortex by thalamic stimulation in patients with chronic pain: a positron emission tomography study. J. Neurosurg. 92, 64–69.

DBS-study-group, 2001. Deep-brain stimulation of the subthalamic nucleus or the pars interna of the globus pallidus in Parkinson's disease. N. Engl. J. Med. 345, 956–963.

Deiber, M.P., Pollak, P., Passingham, R., Landais, P., Gervason, C., Cinotti, L., Friston, K., Frackowiak, R., Mauguiere, F., Benabid, A.L., 1993. Thalamic stimulation and suppression of parkinsonian tremor. Evidence of a cerebellar deactivation using positron emission tomography. Brain 116 (Pt 1), 267–279.

Deuschl, G., Schade-Brittinger, C., Krack, P., Volkmann, J., Schafer, H., Botzel, K., Daniels, C., Deutschlander, A., Dillmann, U., Eisner, W., Gruber, D., Hamel, W., Herzog, J., Hilker, R., Klebe, S., Kloss, M., Koy, J., Krause, M., Kupsch, A., Lorenz, D., Lorenzl, S., Mehdorn, H.M., Moringlane, J.R., Oertel, W., Pinsker, M.O., Reichmann, H., Reuss, A., Schneider, G.H., Schnitzler, A., Steude, U., Sturm, V., Timmermann, L., Tronnier, V., Trottenberg, T., Wojtecki, L., Wolf, E., Poewe, W., Voges, J., 2006. A randomized trial of deep-brain stimulation for Parkinson's disease. N. Engl. J. Med. 355, 896–908.

Doshi, P.K., Chhaya, N., Bhatt, M.H., 2002. Depression leading to attempted suicide after bilateral subthalamic nucleus stimulation for Parkinson's disease. Mov. Disord. 17, 1084–1085.

Dunteman, G.H., 1989. Principal Components Analysis. Sage Publications, Newbury Park.

Felix, B., Leger, M.E., Albe-Fessard, D., Marcilloux, J.C., Rampin, O., Laplace, J.P., 1999. Stereotaxic atlas of the pig brain. Brain Res. Bull. 49, 1–137.

Fields, J.A., Troster, A.I., Wilkinson, S.B., Pahwa, R., Koller, W.C., 1999. Cognitive outcome following staged bilateral pallidal stimulation for the treatment of Parkinson's disease. Clin. Neurol. Neurosurg. 101, 182–188.

Frank, M.J., Samanta, J., Moustafa, A.A., Sherman, S.J., 2007. Hold your horses: impulsivity, deep brain stimulation, and medication in parkinsonism. Science 318, 1309–1312.

Frankemolle, A.M., Wu, J., Noecker, A.M., Voelcker-Rehage, C., Ho, J.C., Vitek, J.L., McIntyre, C.C., Alberts, J.L., 2010. Reversing cognitive-motor impairments in Parkinson's disease patients using a computational modelling approach to deep brain stimulation programming. Brain 133, 746–761.

Funkiewiez, A., Ardouin, C., Caputo, E., Krack, P., Fraix, V., Klinger, H., Chabardes, S., Foote, K., Benabid, A.L., Pollak, P., 2004. Long term effects of bilateral subthalamic nucleus stimulation on cognitive function, mood, and behaviour in Parkinson's disease. J. Neurol. Neurosurg. Psychiatry 75, 834–839.

Ghika, J., Villemure, J.G., Fankhauser, H., Favre, J., Assal, G., Ghika-Schmid, F., 1998. Efficiency and safety of bilateral contemporaneous pallidal stimulation (deep brain stimulation) in levodopa-responsive patients with Parkinson's disease with severe motor fluctuations: a 2-year follow-up review. J. Neurosurg. 89, 713–718.

Grafton, S.T., DeLong, M., 1997. Tracing the brain's circuitry with functional imaging. Nat. Med. 3, 602–603.

Green, A.L., Bittar, R.G., Bain, P., Scott, R.B., Joint, C., Gregory, R., Aziz, T.Z., 2006. STN vs. pallidal stimulation in Parkinson disease: improvement with experience and better patient selection. Neuromodulation 9, 21–27.

Greene, P., 2005. Deep-brain stimulation for generalized dystonia. N. Engl. J. Med. 352, 498–500.

Grill, W.M., Snyder, A.N., Miocinovic, S., 2004. Deep brain stimulation creates an informational lesion of the stimulated nucleus. NeuroReport 15, 1137–1140.

Hardman, C.D., Henderson, J.M., Finkelstein, D.I., Horne, M.K., Paxinos, G., Halliday, G.M., 2002. Comparison of the basal ganglia in rats, marmosets, macaques, baboons, and humans: volume and neuronal number for the output, internal relay, and striatal modulating nuclei. J. Comp. Neurol. 445, 238–255.

Haslinger, B., Boecker, H., Buchel, C., Vesper, J., Tronnier, V.M., Pfister, R., Alesch, F., Moringlane, J.R., Krauss, J.K., Conrad, B., Schwaiger, M., Ceballos-Baumann, A.O., 2003. Differential modulation of subcortical target and cortex during deep brain stimulation. NeuroImage 18, 517–524.

Herzog, J., Reiff, J., Krack, P., Witt, K., Schrader, B., Muller, D., Deuschl, G., 2003. Manic episode with psychotic symptoms induced by subthalamic nucleus stimulation in a patient with Parkinson's disease. Mov. Disord. 18, 1382–1384.

Hilker, R., Voges, J., Ghaemi, M., Lehrke, R., Rudolf, J., Koulousakis, A., Herholz, K., Wienhard, K., Sturm, V., Heiss, W.D., 2003. Deep brain stimulation of the subthalamic

nucleus does not increase the striatal dopamine concentration in parkinsonian humans. Mov. Disord. 18, 41–48.
Houeto, J.L., Mesnage, V., Mallet, L., Pillon, B., Gargiulo, M., du Moncel, S.T., Bonnet, A.M., Pidoux, B., Dormont, D., Cornu, P., Agid, Y., 2002. Behavioural disorders, Parkinson's disease and subthalamic stimulation. J. Neurol. Neurosurg. Psychiatry 72, 701–707.
Jech, R., Urgosik, D., Tintera, J., Nebuzelsky, A., Krasensky, J., Liscak, R., Roth, J., Ruzicka, E., 2001. Functional magnetic resonance imaging during deep brain stimulation: a pilot study in four patients with Parkinson's disease. Mov. Disord. 16, 1126–1132.
Jezzard, P., Clare, S., 1999. Sources of distortion in functional MRI data. Hum. Brain Mapp. 8, 80–85.
Jin, T., Kim, S.G., 2008. Cortical layer-dependent dynamic blood oxygenation, cerebral blood flow and cerebral blood volume responses during visual stimulation. NeuroImage 43, 1–9.
Kalbe, E., Voges, J., Weber, T., Haarer, M., Baudrexel, S., Klein, J.C., Kessler, J., Sturm, V., Heiss, W.D., Hilker, R., 2009. Frontal FDG-PET activity correlates with cognitive outcome after STN-DBS in Parkinson disease. Neurology 72, 42–49.
Kostic, V.S., Agosta, F., Petrovic, I., Galantucci, S., Spica, V., Jecmenica-Lukic, M., Filippi, M., 2010. Regional patterns of brain tissue loss associated with depression in Parkinson disease. Neurology 75, 857–863.
Krack, P., Benazzouz, A., Pollak, P., Limousin, P., Piallat, B., Hoffmann, D., Xie, J., Benabid, A.L., 1998. Treatment of tremor in Parkinson's disease by subthalamic nucleus stimulation. Mov. Disord. 13, 907–914.
Krack, P., Hamel, W., Mehdorn, H.M., Deuschl, G., 1999. Surgical treatment of Parkinson's disease. Curr. Opin. Neurol. 12, 417–425.
Krack, P., Kumar, R., Ardouin, C., Dowsey, P.L., McVicker, J.M., Benabid, A.L., Pollak, P., 2001. Mirthful laughter induced by subthalamic nucleus stimulation. Mov. Disord. 16, 867–875.
Kravitz, A.V., Freeze, B.S., Parker, P.R., Kay, K., Thwin, M.T., Deisseroth, K., Kreitzer, A.C., 2010. Regulation of parkinsonian motor behaviours by optogenetic control of basal ganglia circuitry. Nature 466, 622–626.
Kringelbach, M.L., Jenkinson, N., Owen, S.L., Aziz, T.Z., 2007. Translational principles of deep brain stimulation. Nat. Rev. Neurosci. 8, 623–635.
Kulisevsky, J., Berthier, M.L., Gironell, A., Pascual-Sedano, B., Molet, J., Pares, P., 2002. Mania following deep brain stimulation for Parkinson's disease. Neurology 59, 1421–1424.
Kumar, R., Lozano, A.M., Montgomery, E., Lang, A.E., 1998. Pallidotomy and deep brain stimulation of the pallidum and subthalamic nucleus in advanced Parkinson's disease. Mov. Disord. 13 (Suppl. 1), 73–82.
Lee, J.H., 2012. Informing brain connectivity with optogenetic functional magnetic resonance imaging. NeuroImage (Feb 3, Electronic publication ahead of print).
Lee, K.H., Roberts, D.W., Kim, U., 2003. Effect of high-frequency stimulation of the subthalamic nucleus on subthalamic neurons: an intracellular study. Stereotact. Funct. Neurosurg. 80, 32–36.
Lee, K.H., Chang, S.Y., Roberts, D.W., Kim, U., 2004. Neurotransmitter release from high-frequency stimulation of the subthalamic nucleus. J. Neurosurg. 101, 511–517.
Lee, K.H., Blaha, C.D., Harris, B.T., Cooper, S., Hitti, F.L., Leiter, J.C., Roberts, D.W., Kim, U., 2006. Dopamine efflux in the rat striatum evoked by electrical stimulation of the subthalamic nucleus: potential mechanism of action in Parkinson's disease. Eur. J. Neurosci. 23, 1005–1014.
Limousin, P., Krack, P., Pollak, P., Benazzouz, A., Ardouin, C., Hoffmann, D., Benabid, A.L., 1998. Electrical stimulation of the subthalamic nucleus in advanced Parkinson's disease. N. Engl. J. Med. 339, 1105–1111.
Lozano, A.M., Dostrovsky, J., Chen, R., Ashby, P., 2002. Deep brain stimulation for Parkinson's disease: disrupting the disruption. Lancet Neurol. 1 (4), 225–231.
Mallet, L., Schupbach, M., N'Diaye, K., Remy, P., Bardinet, E., Czernecki, V., Welter, M.L., Pelissolo, A., Ruberg, M., Agid, Y., Yelnik, J., 2007. Stimulation of subterritories of the subthalamic nucleus reveals its role in the integration of the emotional and motor aspects of behavior. Proc. Natl. Acad. Sci. U. S. A. 104, 10661–10666.
Mardia, K.V., Kent, J.T., Bibby, J.M., 1979. Multivariate Analysis. Academic Press, London ; New York.
Martens, H.C., Toader, E., Decre, M.M., Anderson, D.J., Vetter, R., Kipke, D.R., Baker, K.B., Johnson, M.D., Vitek, J.L., 2011. Spatial steering of deep brain stimulation volumes using a novel lead design. Clin Neurophysiol. 122, 558–566.
Masamoto, K., Kim, T., Fukuda, M., Wang, P., Kim, S.G., 2007. Relationship between neural, vascular, and BOLD signals in isoflurane-anesthetized rat somatosensory cortex. Cereb. Cortex 17, 942–950.
McIntyre, C.C., Hahn, P.J., 2010. Network perspectives on the mechanisms of deep brain stimulation. Neurobiol. Dis. 38, 329–337.
McIntyre, C.C., Grill, W.M., Sherman, D.L., Thakor, N.V., 2004a. Cellular effects of deep brain stimulation: model-based analysis of activation and inhibition. J. Neurophysiol. 91, 1457–1469.
McIntyre, C.C., Mori, S., Sherman, D.L., Thakor, N.V., Vitek, J.L., 2004b. Electric field and stimulating influence generated by deep brain stimulation of the subthalamic nucleus. Clin Neurophysiol. 115, 589–595.
Miocinovic, S., Zhang, J., Xu, W., Russo, G.S., Vitek, J.L., McIntyre, C.C., 2007. Stereotactic neurosurgical planning, recording, and visualization for deep brain stimulation in non-human primates. J. Neurosci. Methods 162, 32–41.
Miyawaki, E., Perlmutter, J.S., Troster, A.I., Videen, T.O., Koller, W.C., 2000. The behavioral complications of pallidal stimulation: a case report. Brain Cogn. 42, 417–434.
Montgomery Jr., E.B., Gale, J.T., 2008. Mechanisms of action of deep brain stimulation (DBS). Neurosci. Biobehav. Rev. 32, 388–407.
Moum, S.J., Price, C.C., Limotai, N., Oyama, G., Ward, H., Jacobson, C., Foote, K.D., Okun, M.S., 2012. Effects of STN and GPi deep brain stimulation on impulse control disorders and dopamine dysregulation syndrome. PLoS One 7, e29768.
Nielsen, M.S., Sorensen, J.C., Bjarkam, C.R., 2009. The substantia nigra pars compacta of the Gottingen minipig: an anatomical and stereological study. Brain Struct. Funct. 213, 481–488.
Okun, M.S., Foote, K.D., 2005. Subthalamic nucleus vs globus pallidus interna deep brain stimulation, the rematch: will pallidal deep brain stimulation make a triumphant return? Arch. Neurol. 62, 533–536.
Okun, M.S., Tagliati, M., Pourfar, M., Fernandez, H.H., Rodriguez, R.L., Alterman, R.L., Foote, K.D., 2005. Management of referred deep brain stimulation failures: a retrospective analysis from 2 movement disorders centers. Arch. Neurol. 62, 1250–1255.
Phillips, M.D., Baker, K.B., Lowe, M.J., Tkach, J.A., Cooper, S.E., Kopell, B.H., Rezai, A.R., 2006. Parkinson disease: pattern of functional MR imaging activation during deep brain stimulation of subthalamic nucleus–initial experience. Radiology 239, 209–216.
Pictet, J., Meuli, R., Wicky, S., van der Klink, J.J., 2002. Radiofrequency heating effects around resonant lengths of wire in MRI. Phys. Med. Biol. 47, 2973–2985.
Pour-El, I., 2006. Animals in translation: using the mysteries of autism to decode animal behavior. Libr. J. 131, 119-119.
Reijnders, J.S., Scholtissen, B., Weber, W.E., Aalten, P., Verhey, F.R., Leentjens, A.F., 2010. Neuroanatomical correlates of apathy in Parkinson's disease: a magnetic resonance imaging study using voxel-based morphometry. Mov. Disord. 25, 2318–2325.
Rezai, A.R., Lozano, A.M., Crawley, A.P., Joy, M.L., Davis, K.D., Kwan, C.L., Dostrovsky, J.O., Tasker, R.R., Mikulis, D.J., 1999. Thalamic stimulation and functional magnetic resonance imaging: localization of cortical and subcortical activation with implanted electrodes. Technical note. J. Neurosurg. 90, 583–590.
Rezai, A.R., Finelli, D., Nyenhuis, J.A., Hrdlicka, G., Tkach, J., Sharan, A., Rugieri, P., Stypulkowski, P.H., Shellock, F.G., 2002. Neurostimulation systems for deep brain stimulation: in vitro evaluation of magnetic resonance imaging-related heating at 1.5 tesla. J. Magn. Reson. Imaging 15, 241–250.
Rezai, A.R., Baker, K.B., Tkach, J.A., Phillips, M., Hrdlicka, G., Sharan, A.D., Nyenhuis, J., Ruggieri, P., Shellock, F.G., Henderson, J., 2005. Is magnetic resonance imaging safe for patients with neurostimulation systems used for deep brain stimulation. Neurosurgery 57, 1056–1062 (discussion 1056–1062).
Romito, L.M., Raja, M., Daniele, A., Contarino, M.F., Bentivoglio, A.R., Barbier, A., Scerrati, M., Albanese, A., 2002. Transient mania with hypersexuality after surgery for high frequency stimulation of the subthalamic nucleus in Parkinson's disease. Mov. Disord. 17, 1371–1374.
Saikali, S., Meurice, P., Sauleau, P., Eliat, P.A., Bellaud, P., Randuineau, G., Verin, M., Malbert, C.H., 2010. A three-dimensional digital segmented and deformable brain atlas of the domestic pig. J. Neurosci. Methods 192, 102–109.
Saint-Cyr, J.A., Trepanier, L.L., Kumar, R., Lozano, A.M., Lang, A.E., 2000. Neuropsychological consequences of chronic bilateral stimulation of the subthalamic nucleus in Parkinson's disease. Brain 123 (Pt 10), 2091–2108.
Shon, Y.M., Lee, K.H., Goerss, S.J., Kim, I.Y., Kimble, C., Van Gompel, J.J., Bennet, K., Blaha, C.D., Chang, S.Y., 2010. High frequency stimulation of the subthalamic nucleus evokes striatal dopamine release in a large animal model of human DBS neurosurgery. Neurosci. Lett. 475, 136–140.
Smith, S.M., Jenkinson, M., Woolrich, M.W., Beckmann, C.F., Behrens, T.E., Johansen-Berg, H., Bannister, P.R., De Luca, M., Drobnjak, I., Flitney, D.E., Niazy, R.K., Saunders, J., Vickers, J., Zhang, Y., De Stefano, N., Brady, J.M., Matthews, P.M., 2004. Advances in functional and structural MR image analysis and implementation as FSL. NeuroImage 23 (Suppl. 1), S208–S219.
Starr, P.A., Christine, C.W., Theodosopoulos, P.V., Lindsey, N., Byrd, D., Mosley, A., Marks Jr., W.J., 2002. Implantation of deep brain stimulators into the subthalamic nucleus: technical approach and magnetic resonance imaging-verified lead locations. J. Neurosurg. 97, 370–387.
Stefurak, T., Mikulis, D., Mayberg, H., Lang, A.E., Hevenor, S., Pahapill, P., Saint-Cyr, J., Lozano, A., 2003. Deep brain stimulation for Parkinson's disease dissociates mood and motor circuits: a functional MRI case study. Mov. Disord. 18, 1508–1516.
Strafella, A.P., Sadikot, A.F., Dagher, A., 2003. Subthalamic deep brain stimulation does not induce striatal dopamine release in Parkinson's disease. NeuroReport 14, 1287–1289.
Tarsy, D., 2008. Deep Brain Stimulation in Neurological and Psychiatric Disorders. Humana Press, Totowa, NJ.
Trepanier, L.L., Kumar, R., Lozano, A.M., Lang, A.E., Saint-Cyr, J.A., 2000. Neuropsychological outcome of GPi pallidotomy and GPi or STN deep brain stimulation in Parkinson's disease. Brain Cogn. 42, 324–347.
Ulla, M., Thobois, S., Lemaire, J.J., Schmitt, A., Derost, P., Broussolle, E., Llorca, P.M., Durif, F., 2006. Manic behaviour induced by deep-brain stimulation in Parkinson's disease: evidence of substantia nigra implication? J. Neurol. Neurosurg. Psychiatry 77, 1363–1366.
Van Gompel, J.J., Bower, M.R., Worrell, G.A., Stead, M., Meier, T.R., Goerss, S.J., Chang, S.Y., Kim, I., Meyer, F.B., Richard Marsh, W., Marsh, M.P., Lee, K.H., 2011. Swine model for translational research of invasive intracranial monitoring. Epilepsia 52, e49–e53.
Vingerhoets, G., van der Linden, C., Lannoo, E., Vandewalle, V., Caemaert, J., Wolters, M., Van den Abbeele, D., 1999. Cognitive outcome after unilateral pallidal stimulation in Parkinson's disease. J. Neurol. Neurosurg. Psychiatry 66, 297–304.
Vitek, J.L., 2002a. Deep brain stimulation for Parkinson's disease. A critical re-evaluation of STN versus GPi DBS. Stereotact. Funct. Neurosurg. 78, 119–131.
Vitek, J.L., 2002b. Mechanisms of deep brain stimulation: excitation or inhibition. Mov. Disord. 17 (Suppl. 3), S69–S72.
Voon, V., Kubu, C., Krack, P., Houeto, J.L., Troster, A.I., 2006. Deep brain stimulation: neuropsychological and neuropsychiatric issues. Mov. Disord. 21 (Suppl. 14), S305–S327.
Wakeman, D.R., Crain, A.M., Snyder, E.Y., 2006. Large animal models are critical for rationally advancing regenerative therapies. Regen. Med. 1, 405–413.
Weaver, F.M., Follett, K.A., Stern, M., Luo, P., Harris, C.L., Hur, K., Marks Jr., W.J., Rothlind, J., Sagher, O., Moy, C., Pahwa, R., Burchiel, K., Hogarth, P., Lai, E.C.,

Duda, J.E., Holloway, K., Samii, A., Horn, S., Bronstein, J.M., Stoner, G., Starr, P.A., Simpson, R., Baltuch, G., De Salles, A., Huang, G.D., Reda, D.J., 2012. Randomized trial of deep brain stimulation for Parkinson disease: thirty-six-month outcomes. Neurology 79, 55–65.

Witt, K., Daniels, C., Reiff, J., Krack, P., Volkmann, J., Pinsker, M.O., Krause, M., Tronnier, V., Kloss, M., Schnitzler, A., Wojtecki, L., Botzel, K., Danek, A., Hilker, R., Sturm, V., Kupsch, A., Karner, E., Deuschl, G., 2008. Neuropsychological and psychiatric changes after deep brain stimulation for Parkinson's disease: a randomised, multicentre study. Lancet Neurol. 7, 605–614.

Wu, Y.R., Levy, R., Ashby, P., Tasker, R.R., Dostrovsky, J.O., 2001. Does stimulation of the GPi control dyskinesia by activating inhibitory axons? Mov. Disord. 16, 208–216.